

Moon night sky brightness simulation for the Xinglong station

Song Yao^{1,2}, Hao-Tong Zhang¹, Hai-Long Yuan¹, Yong-Heng Zhao¹, Yi-Qiao Dong¹,
Zhong-Rui Bai¹, Li-Cai Deng¹ and Ya-Juan Lei¹

¹ Key Laboratory of Optical Astronomy, National Astronomical Observatories, Chinese Academy of Sciences, Beijing 100012, China; zht@lamost.org

² Graduate University of Chinese Academy of Sciences, Beijing 100049, China

Received 2013 February 26; accepted 2013 April 16

Abstract Using a sky brightness monitor at the Xinglong station of National Astronomical Observatories, Chinese Academy of Sciences, we collected data from 22 dark clear nights and 90 moon nights. We first measured the sky brightness variation with time for dark nights and found a clear correlation between sky brightness and human activity. Then with a modified sky brightness model of moon nights and data from these nights, we derived the typical value for several important parameters in the model. With these results, we calculated the sky brightness distribution under a given moon condition for the Xinglong station. Furthermore, we simulated the sky brightness distribution of a moon night for a telescope with a 5° field of view (such as LAMOST). These simulations will be helpful for determining the limiting magnitude and exposure time, as well as planning the survey for LAMOST during moon nights.

Key words: Moon — scattering — site testing — telescopes

1 INTRODUCTION

The night sky brightness of an observatory is the major factor that constrains the limiting magnitude of a telescope and the exposure time given the required signal-to-noise ratio of the targets. For a spectral instrument using fibers, sky subtraction is a crucial step in reducing the spectral data taken with fibers; usually this step relies on how the fiber samples the background, which is generally thought to be homogenous within 1° on dark nights. If there is a gradient in the sky background (such as on a moon night), much more effort will be needed in both designing the fiber used for sky sampling and the method of data reduction. Thus a good estimation of sky background distribution is very important in planning a spectroscopic survey that uses fibers and has a large field of view, such as the Large sky Area Multi-Object fiber Spectroscopic Telescope (LAMOST, also called the Guo Shou Jing Telescope, Cui et al. 2012).

There are several sources that contribute to light in the night sky after astronomical twilight, namely airglow, scattering of starlight and zodiacal light, and natural and artificial light pollution. For an astronomical observatory, artificial light pollution is generally very small and the most dominant source of light pollution is moonlight when the moon is above the horizon. Many previous works have studied the night sky brightness, for example: Sánchez et al. (2007), Schneeberger et al. (1979) and Neugent & Massey (2010). However, most of these papers focus on dark night sky brightness, and only a few of them study the sky brightness on moon nights. The site for LAMOST

is the Xinglong Station of the National Astronomical Observatories, Chinese Academy of Sciences (NAOC), which is located 114 km northeast of Beijing at a longitude of $7^{\text{h}}50^{\text{m}}18^{\text{s}}$ east, a latitude of $40^{\circ}23'36''$ north, and an altitude of about 900 m. Liu et al. (2003) and Yao et al. (2012) studied the night sky brightness, seeing, extinction, and available observational hours as well as their seasonal changes using photometric data from the telescope used for the Beijing-Arizona-Taiwan-Connecticut (BATC) survey, which is located at the Xinglong Station. For the night sky during a moon night, they used a simple empirical model considering the moon's phase, height and angular distance between the moon and the target to eliminate the effect of the moon. The model used in their paper is too simple to estimate the sky brightness distribution in detail over a 5° field of view (for LAMOST). Krisciunas & Schaefer (1991) derived a more complicated model considering both the Rayleigh and Mie scattering of the moonlight; two more variables, zenith distance of the moon and zenith distance of the target, were considered in their model, and the reported accuracy was 8%–23%. In the present work, with a modified model of sky brightness during a moon night from Krisciunas & Schaefer (1991) and using data from a Sky Quality Meter (SQM) at the Xinglong station, we derived typical values for several important parameters. With these results, we calculated the sky brightness distribution under a given moon condition. Furthermore, we use these results to predict the typical brightness gradient for LAMOST's 5° field of view.

In Section 2 we describe the model of sky brightness. In Section 3 the process of how we derived data describing the brightness measurement from the SQM is explained. In Section 4 we present the fitting of parameters, including the dark zenith sky brightness V_{zen} , the extinction coefficient k , and the scattering coefficients PA and PB. In Section 5 we calculate the sky brightness distribution when the moon is at a specific position and phase angle, using typical values of the deduced sky parameters. Furthermore, the variation in brightness distribution over a 5° field of view that is caused by the moon is predicted and its effect on LAMOST is discussed.

2 CALCULATION MODEL

According to Krisciunas & Schaefer (1991), the sky brightness on a moon night can be divided into two parts, the dark nighttime sky

$$B_0(B_{\text{zen}}, k, z) = B_{\text{zen}} 10^{-0.4k(X-1)} X, \quad (1)$$

and the contribution from scattered moonlight

$$B_{\text{moon}} = f(\rho) I^* 10^{-0.4kX_m(Z_m)} (1 - 10^{-0.4kX(Z)}), \quad (2)$$

where B_{zen} is the dark time sky brightness at zenith in nanoLamberts (nL) which can be converted to magnitude V_{zen} with equation (27) in Garstang (1989), k is the extinction coefficient, $f(\rho)$ is the scattering function at scattering angle ρ , I^* is the brightness of the moon outside the atmosphere, which can be expressed as a function of moon phase angle α

$$I^* = 10^{-0.4(3.84+0.026|\alpha|+4 \times 10^{-9}\alpha^4)}, \quad (3)$$

Z is the zenith distance, X is the airmass and $X_m(Z_m)$ and $X(Z)$ denote the airmass for the moon and the sky position respectively. The airmass X can be expressed as in Garstang (1989)

$$X(Z) = (1 - 0.96 \sin^2 Z)^{-0.5}. \quad (4)$$

The scattering function is composed of two types of scattering in the atmosphere, Rayleigh scattering from atmospheric gases and Mie scattering by atmospheric aerosols. The Mie scattering can degenerate into Rayleigh scattering when the size of atmospheric aerosols decreases. However, when the size increases, the behavior of the scattering can be described by geometrical optics. The scattering function is proportional to the fraction of incident light scattered into a unit solid angle with

a scattering angle, and also varies with different wavelengths. According to Krisciunas & Schaefer (1991) and Chakraborty et al. (2005), we define the scattering functions as

$$f_R(\rho) = 10^{5.36}(1.06 + \cos^2 \rho), \quad (5)$$

$$f_M(\rho) = 10^{6.15 - \frac{\rho}{40}}, \quad \text{when } (\rho \geq 10), \quad (6)$$

$$f_M(\rho) = 6.2 \times 10^7 \rho^{-2}, \quad \text{when } (\rho \leq 10), \quad (7)$$

$$f(\rho) = PA \times f_M(\rho) + PB \times f_R(\rho). \quad (8)$$

In these functions, $f_R(\rho)$ and $f_M(\rho)$ are the Rayleigh and Mie scattering functions respectively. ρ is the scattering angle defined as the angular separation between the moon and the sky position. In Equation (8), PA is a scale factor for Mie scattering and PB is a scale factor for Rayleigh scattering; they are proportional to the density of particles that experience Mie and Rayleigh scattering in the atmosphere. In Krisciunas & Schaefer (1991), the scattering function (eq. (16) in that paper) includes a constant factor relating to unit conversions and normalizations. Since the particle densities may change with time and weather conditions from site to site, we use PA and PB as scale factors to scale the relative particle density to the site (Mauna Kea) used in that paper, and they were treated as free parameters rather than fixed values in the data fitting program in Section 4 to deal with different weather conditions. If the scattering angle is small, the moonlight can directly enter the measurement instrument and Equation (5) is not applicable in that case.

Finally, the sky brightness during a moon night can be simply expressed as

$$B = B_0 + B_{\text{moon}}. \quad (9)$$

Here, B_0 is the dark night sky brightness in Equation (1) and B_{moon} is the brightness caused by the moonlight in Equation (2). Combining all the equations above, the sky brightness can be expressed as

$$B = B(B_{\text{zen}}, k, Z_{\text{moon}}, Z_{\text{sky}}, \rho, \alpha, PA, PB). \quad (10)$$

Here B_{zen} is the dark zenith sky brightness in nL; k is the extinction coefficient; Z_{moon} is the moon zenith distance; Z_{sky} is the zenith distance of the sky position; ρ is the scattering angle; α is the moon phase angle; PA is the Mie scattering scale factor; PB is the Rayleigh scattering scale factor.

The motions of the moon can be calculated using Chapront ELP-2000/82 (Meeus 1991). The corresponding equatorial coordinates (RA, DEC) describing its position can then be obtained. For application in this paper, the accuracy given by the mean position of the moon is enough. The Greenwich Mean Sidereal Time can be calculated as

$$\text{GMST} = 100.46061837 + 36000.770053608T + 0.000387933T^2 - T^3/38710000. \quad (11)$$

Here T is the date in Julian centuries starting from J2000.0. Then the hour angle of the moon can be calculated as

$$H_{\text{local}} = \text{GMST} - \text{RA} - \text{LON}. \quad (12)$$

Here the geographic longitude (LON) is 117.575703° and the geographic latitude (LAT) is 40.3933333° . The azimuth angle (A) and the elevation angle (h) of the moon can then be calculated as

$$\begin{cases} \sin h = \sin \text{LAT} \sin \text{DEC} + \cos \text{LAT} \cos \text{DEC} \cos H_{\text{local}}, \\ \cos h \cos A = \cos \text{LAT} \sin \text{DEC} - \sin \text{LAT} \cos \text{DEC} \cos H_{\text{local}}, \\ \cos h \sin A = -\cos \text{DEC} \sin H_{\text{local}}. \end{cases} \quad (13)$$

3 SKY BRIGHTNESS DATA IN THE XINGLONG

The SQM (see <http://www.uni-hedron.com/projects/darksky/>) is a handy tool developed by the Uni-hedron company to measure the sky brightness of visual light in mag arcsec^{-2} . There is a filter that blocks near-infrared radiation from entering the fiber to constrain the light to the visual band. The transmission curve describing the transmitted light associated with the SQM can be found in figure 22 of Cinzano (2005) (<http://www.lightpollution.it/download/sqmreport.pdf>); the wavelength response is very broad, with the half maximum of the sensitivity curve being in the range from 4000 to 6000 Å and the peak at 5400 Å. Due to the broadness of the response, the conversion to the Johnson V band will depend on the spectral type. But for a measure of sky brightness during a dark night or moonlight, the magnitude of the SQM is similar to that in the V band, with an error of about 0.1 mag (Cinzano 2005). Each SQM is calibrated by a light meter with a NIST-traceable calibration, and the absolute precision of each meter is manufactured to be 10% ($0.1 \text{ mag arcsec}^{-2}$). The difference in zero point between each calibrated SQM is also 10% ($0.1 \text{ mag arcsec}^{-2}$). Adding the above errors together, the overall sky brightness measured in the V band is about $0.2 \text{ mag arcsec}^{-2}$.

An SQM was installed at the Xinglong station of NAOC. During the course of this study, it measured the sky brightness in magnitude per square arcsecond every 6 min for more than a year. The Full Width at Half Maximum of the angular sensitivity is $\sim 20^\circ$. The SQM is fixed in a metal framework and will not change its direction until it is manually shifted.

Table 1 shows the direction of SQM in degrees during the days when the data were collected.

Table 1 Direction of the SQM

Start date	End date	Azimuth ($^\circ$)	Zenith distance ($^\circ$)
2010-12-16	2011-12-14	180 (South)	15
2011-12-15	2012-01-12	180 (South)	30
2012-01-13	2012-02-13	90 (East)	30
2012-02-14	2012-03-12	0 (North)	30

Notes: the azimuth zero point is north and the clockwise direction is positive.

To measure the sky brightness on dark nights, we select data from nights around the new moon when the moon is below the horizon, then we look up the observation log of LAMOST to reject those nights that were not marked as a clear night, which gives us about 22 nights. It will be interesting to explain how those data were influenced by light pollution from nearby cities and solar activities, but as we only have a few nights for each direction in Table 1, and most data were acquired during the winter, it is hard to tell how artificial light influenced the detailed pattern of dark nighttime sky brightness. We still need time to accumulate more data to find the nightly pattern with seasons and directions. So, here we only show the average dark night brightness with time. We first correct the sky brightness to the value at zenith with Equation (1), then we set midnight as the fiducial time. The data from different nights were then averaged every 10 min from the fiducial. The results are plotted in Figure 1. There is a clear tendency that the sky brightness is brighter in the first half of the night, but after midnight the sky brightness gets darker by about 0.3 mag. This may be explained by human activities decreasing after midnight, so the light pollution is reduced for the second half of the night. The overall dark night sky brightness is about $21.6 \pm 0.2 \text{ mag arcsec}^{-2}$. The error bar for each data point in Figure 1 should reflect both the stability of the instrument and the nightly change of the sky conditions. By comparing with the scatter in sky brightness, which is on the order of 0.4 mag in Liu et al. (2003), and considering that our data were obtained in a period of about one year, the dominate contributor to this error bar should be the sky itself; the stability of the SQM should be much smaller than 0.2 mag.

The direction of the SQM was adjusted with simple tools so measurements are accurate over a range of several square degrees. Those data were taken over more than 400 d with all kinds of

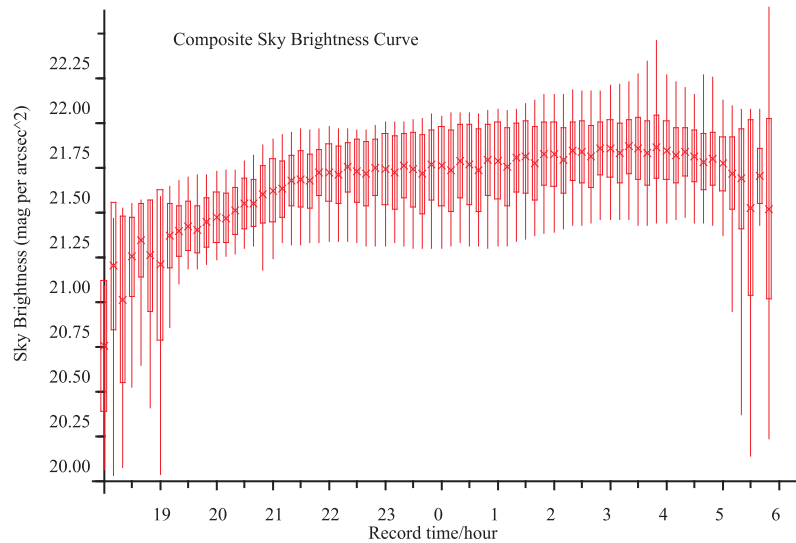


Fig. 1 The average sky brightness during night time from 22 possible clear dark nights. The vertical box at each data point shows a 1σ error bar, and the vertical solid lines indicate the maximum and minimum value of that data point. There is a clear tendency that the night sky brightness is brighter in the first half of the night, and it becomes darker in the second half due to less human activity.

weather conditions, such as days with heavy clouds. Also, there is no guarantee that the weather should be stable during one night. To measure the sky brightness of scattered moonlight, we need to exclude those situations in which the scattering model cannot work properly, so we use several rules to filter the data set:

- (1) Exclude the daytime records according to astronomical twilight.
- (2) Exclude the records when the altitude of the moon is less than 5° .
- (3) Exclude the records when the angular distance from the moon is smaller than 32.5° , or the sky brightness is brighter than 18 (mag arcsec^{-2}) to avoid direct incidence of moonlight.
- (4) Exclude the observational nights whose record of counts is smaller than 25 to avoid nights with heavy clouds.
- (5) Exclude the observation nights whose observed brightness curves show an irregular transition or dispersion larger than 30% to avoid drastic weather changes or partial cloud blocking.

In the end, we obtained sky brightness data for 114 moon nights from 2010 December 16 to 2012 March 12. Each night when observations were taken contains about 42 records.

4 PARAMETER FITTING

The following work is mainly based on Equation (10). Here the zenith distance of the moon Z_{moon} , the zenith distance of the sky position Z_{sky} , the angular separation between the moon and the sky position ρ and the moon phase angle α in degrees are taken as input arguments, since they can be calculated from the observatory's geographical location and time. The dark zenith sky brightness V_{zen} , the extinction coefficient k , the Mie scattering scale factor PA and the Rayleigh scattering scale factor PB are treated as parameters to be determined. The output result is sky brightness in nanoLamberts, which is provided through measurements with the SQM.

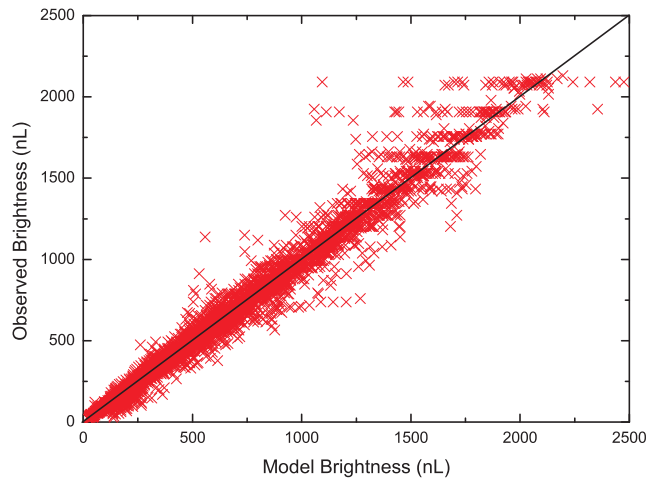


Fig. 2 The model brightness versus the observed brightness. About 5200 data records from 114 nights are presented. The total relative fitting variation defined by Eq. (15) is 12%.

In order to solve the non-linear least squares problem, we collect the observed sky brightness records on each observation night as one data set. The number of data records (N) in each data set is approximately 42. Using information about the observatory's geographical location and time, input values for the moon and sky position can be estimated and attached to each record. It is assumed that for one night the parameters (V_{zen} , k , PA and PB) do not change very much so they are treated as constants. We can determine the value of these parameters for each night that will give a minimum value of the squared 2-norm residual, which is defined as

$$\text{RESNORM} = \sum_{i=1}^{i=N} (\text{Model}B_i - \text{Observed}B_i)^2. \quad (14)$$

The initial values of the parameters (V_{zen} , k , PA and PB) are set as 21.4, 0.23, 1 and 1 respectively. The magnitude at zenith is limited between 0 and 25; the extinction coefficient is constrained between 0.01 and 8; the parameters PA and PB are constrained between 0 and 25. Finally we obtained the fitting results for 114 data sets. If we reject data sets with parameters that are returned at or close to the boundary for constraints, 90 data sets remain.

Figure 2 shows the model brightness versus the measured brightness for the data records of all the data sets from 114 nights, which contain more than 5000 records. We define the relative fitting variation (RFV) as

$$\text{RFV} = \sqrt{\frac{1}{N} \sum_{i=1}^{i=N} \left(\frac{\text{Model}B_i - \text{Observed}B_i}{\text{Observed}B_i} \right)^2}. \quad (15)$$

The total relative fitting variation defined by Equation (15) and plotted in Figure 2 is 12%. The RFVs for each data set are shown in Figure 3. Only the last 90 data sets are presented. As we can see, most of the fitting results have an RFV smaller than 5%. That means for most of the remaining nights, the brightness predicted by the model matches the observed brightness with high accuracy.

Figure 4 shows examples of the fitting curve from four nights. Here, the phase angle of the moon is expressed as the Sun-Moon-Earth angle in degrees. Values in RFV are 2.9%, 4.7%, 3.5% and 10%, as marked in the figure. It is obvious that the bottom-right figure has the maximum brightness because the phase angle is the smallest among the four figures, and the top-right one has the minimum

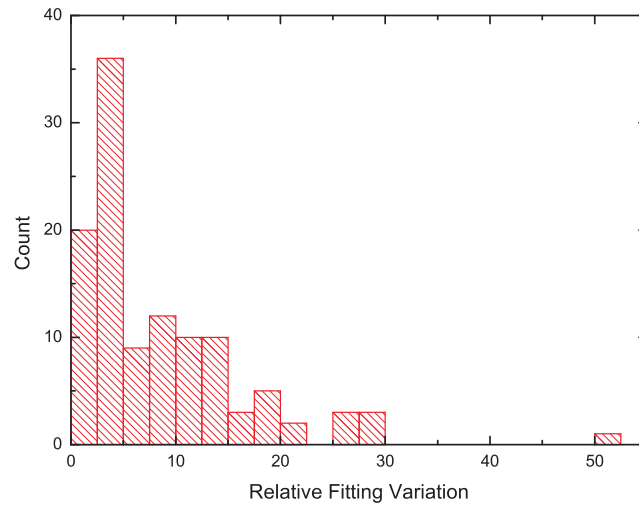


Fig. 3 Histogram of relative fitting variation of each observation night. Only the the last 90 nights are presented. Most of the variations are smaller than 5%.

brightness. The major influencing factor of the trend in the curve is the angular separation between the moon and the sky position. As we can see from these figures, when the moon moves close to the sky position, the sky background becomes bright. Since the sky direction and the moon's declination for one night are basically fixed, the angular separation is determined by the moon's altitude. Eventually when the moon is on the meridian, the background in the field of view of a quasi-meridian telescope, such as LAMOST, will be very bright. These results show that this fitting model works well for various phase angles and locations of the moon.

Nights with bad fitting results are due to the following reasons:

- (1) The weather conditions. As this measurement instrument has worked without interruption for years, the data have been produced on days with various kinds of weather conditions. These effects cannot be corrected using the presented models.
- (2) The large angular sensitivity of the SQM. Within that large field of view, the light from stars and planets, and especially moonlight when the moon is close, will greatly affect the measurement results. Consequently, the measured sky brightness shows a sharp increase as the moon moves close to the sky position.
- (3) The reflection of moonlight from the surrounding buildings.
- (4) The light pollution from nearby cities. The sky brightness of the Xinglong station is mainly polluted by city lights from Beijing, Xinglong and Chengde. As we can see from Figure 1, the artificial light pollution can change the sky brightness by about 0.3 mag at night. Those effects are ignored in the model since the sky brightness we are considering is at least one magnitude brighter than the dark night. The sky brightness in the absence of moonlight is expressed by Equation (1).

After iterative fitting, the resulting histogram of the estimated parameters, including the dark zenith sky brightness V_{zen} , extinction coefficient k and scattering coefficients PA and PB, are shown in Figure 5. Only the last 90 data sets are presented. The dark zenith sky brightness, V_{zen} , presents a typical value of 21.4 mag arcsec⁻². This result agrees with the zenith sky brightness (21.6 ± 0.2 mag arcsec⁻²) in the winter that we measured from dark nights, given in Section 3. This also

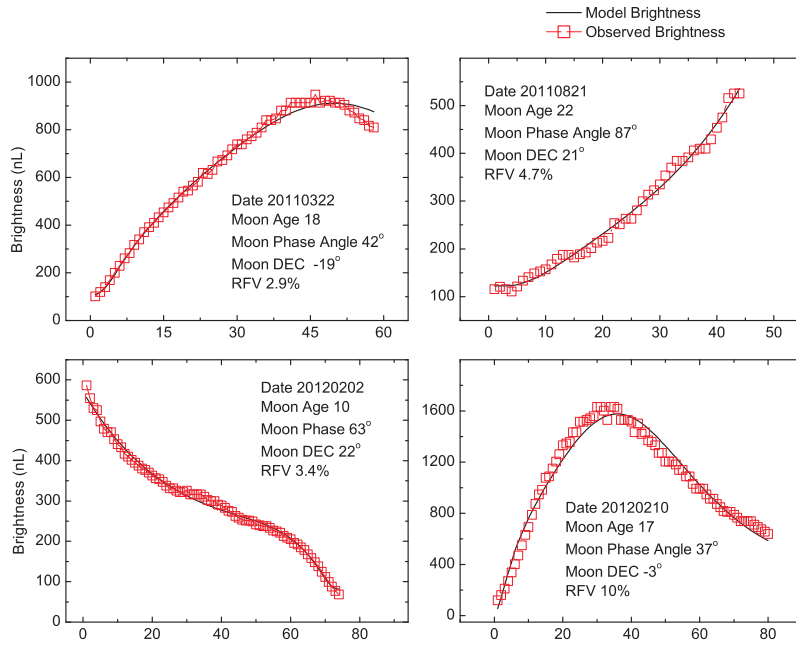


Fig. 4 Sky brightness fitting curves. The X axis is the serial number for the measured data point. Related parameters, including observation date, moon age, moon phase angle in degrees, moon declination and relative fitting variation RFV, are printed in the figures. The definition of RFV is described in Eq. (15). The SQM directions are listed in Table 1.

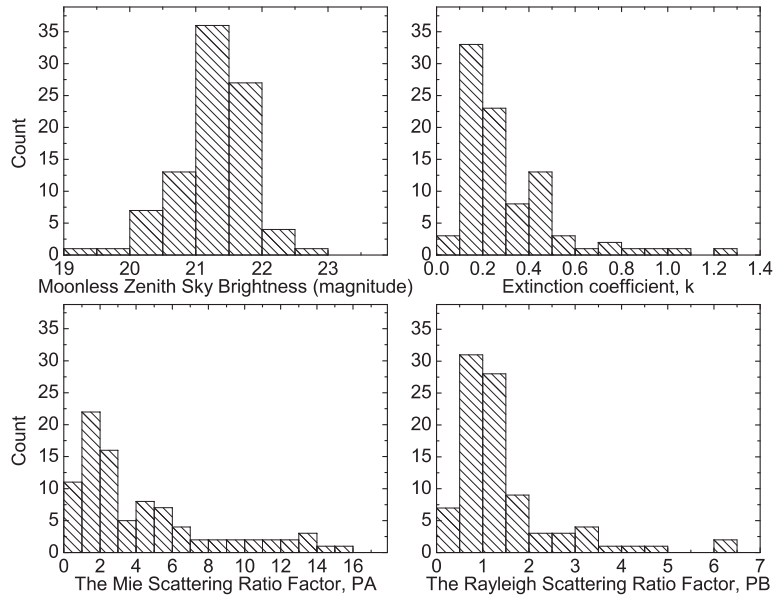


Fig. 5 Histogram of the estimated parameters, including the dark zenith sky brightness V_{zen} , extinction coefficient k , and scattering coefficients PA and PB. Only the last 90 data sets are presented. Typical values for these parameters can be read from the figures as: $V_{zen} = 21.4$, $k = 0.23$, PA = 1.5 and PB = 0.90.

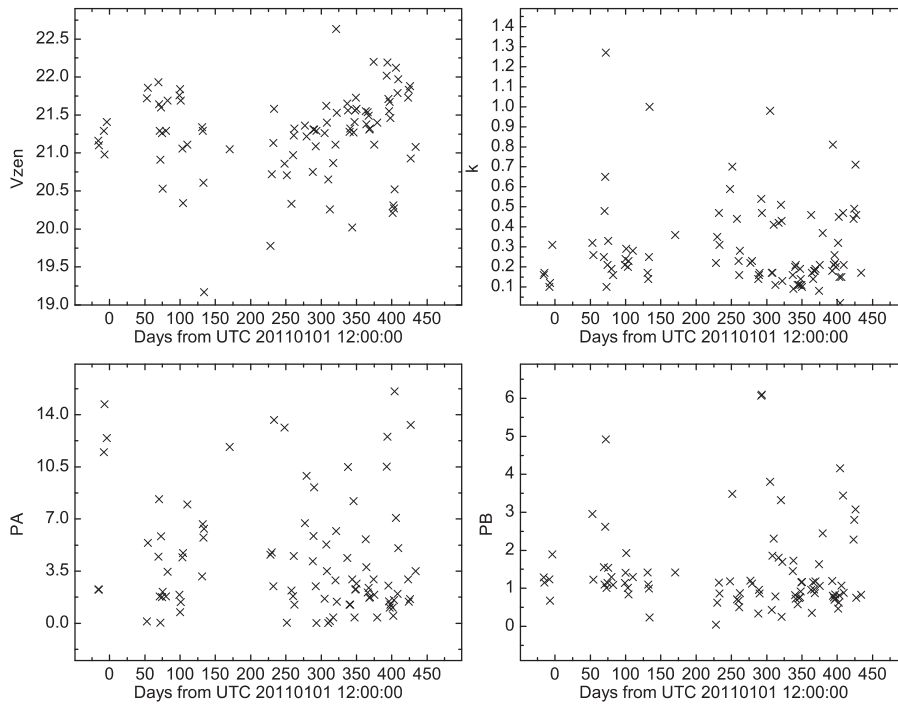


Fig. 6 Estimated parameters as a function of date. Top left: zenith sky brightness versus time. Top right: extinction vs. time. Bottom left: Mie scattering factor PA vs. time. Bottom right: Rayleigh scattering factor PB vs. time. Only the last 90 data sets are presented. The days are calculated starting from 2011 January 1, 12:00:00. Days close to 0 or 365.25 are in the winter. Days near 180 are in the summer.

basically fits the sky brightness in the V band obtained from BATC Polaris monitoring data (Yao et al. 2012), which is about $21 \text{ mag arcsec}^{-2}$ at the North Celestial Pole. Correcting the airmass using Equation (1) with 0.36 mag, the results agree very well. The extinction coefficient, k , has a typical value of 0.23. This is in the acceptable range according to the measurement results at Xinglong (Liu et al. 2003; Yao et al. 2012). The scale factor for Mie scattering, PA, shows a typical value of 1.50. The scale factor for Rayleigh scattering, PB, presents a typical value of 0.90.

Figure 6 displays the estimated parameters as a function of date from 2011 January 1. The data were collected within one year, and there is an obvious lack of data in the summer due to the bad weather. Since there are not enough data, it is hard to tell how parameters describing the system change with seasons. However, we can still find some indications that the zenith is darker in the winter than in the summer and the sky transparency in the autumn and winter is better than those in the spring and summer, which is also consistent with previous work, e.g. Liu et al. (2003) and Yao et al. (2012). However, the scattering scale factors PA and PB show no obvious seasonal variation. The factor PA has a larger dispersion than PB. This is mainly because the density of the Mie scattering particles (i.e. dust) has a bigger variation than molecules that cause Rayleigh scattering. More data are needed to better resolve how these parameters change with seasons.

Liu et al. (2003) found a linear relation between the sky brightness and extinction coefficient k . However, in our results (see Fig. 7), this correlation is not found. Since the data in the Liu et al. (2003) paper were collected around Polaris, there is a fixed zenith distance at about 50° in the Xinglong

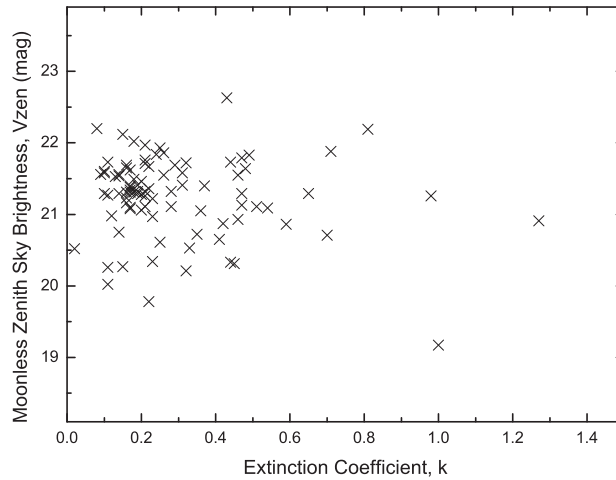


Fig. 7 Extinction coefficient k vs. zenith sky brightness V_{zen} .

station. Considering Equation (1), we conclude that the linear correlation agrees with the equation but the measured sky brightness is NOT the zenith brightness.

5 SKY BRIGHTNESS DISTRIBUTION

5.1 Sky Brightness Estimation

Estimation of sky background is important for a telescope working during a moon night. The background brightness is one of the key factors that determine the limiting magnitude and exposure time. For a survey telescope working during a moon night, knowing the background distribution will help astronomers to plan how far from the moon the telescope should point in order to reduce the influence of the moon. By applying the typical parameters from fitting results to Equation (10), we can calculate the sky brightness for the Xinglong station given sky position and time during a moon night, except for the region where the moon is very close to the sky position ($< 10^\circ$). Here we give two examples in Tables 2 and 3.

In Table 2 the moon is assumed to have a phase angle of 20° , an hour angle of -30° and a declination of -10° . The brightness distribution is presented in a large region with an hour angle from -35° to 35° and declination from -10° to 70° . For an intuitive view, the sky brightness distribution for moon phase angle 20° , declination -20° and hour angle -30° is plotted in Figure 8.

Table 3 is for a moon on the meridian with a phase angle of 90° and declination of 20° . The position within 10° of the moon was left blank in the table. The brightness in Tables 2 and 3 will be used to set the current magnitude limit and estimate exposure time for the LAMOST survey in each moon night. They could also help to determine where the telescope should point for a given scientific request. For example, to reach magnitude 17 on a bright night, the background should be no brighter than $19 \text{ mag arcsec}^{-2}$.

In Table 2 and Figure 8, when the moon's phase is close to full, the sky position should be at least 65° away to reach a limit of $19 \text{ mag arcsec}^{-2}$; by comparing with Table 3 when the moon is half illuminated, the sky is as deep as $19 \text{ mag arcsec}^{-2}$ when the sky position is 15° from the moon. From Tables 2, 3 and Figure 8, we can see that the brightness gradient is larger when the telescope is pointing closer to the moon. The sky brightness drops faster in the declination direction than in

Table 2 The sky brightness distribution at the Xinglong station when the moon is 2 hours before the transit. The brightness is in the V band and expressed as mag arcsec^{-2} . Input conditions are listed below the table.

Dec\h	-35	-30	-25	-20	-15	-10	-5	0	5	10	15	20	25	30	35
-10		Moon			17.16	17.39	17.59	17.77	17.93	18.08	18.20	18.30	18.38	18.45	18.49
-5				17.06	17.29	17.50	17.70	17.88	18.03	18.17	18.29	18.40	18.48	18.55	18.60
0	17.02		17.10	17.27	17.45	17.64	17.83	17.99	18.14	18.28	18.39	18.49	18.58	18.64	18.69
5	17.29	17.30	17.37	17.50	17.65	17.81	17.97	18.12	18.26	18.38	18.49	18.59	18.67	18.73	18.78
10	17.55	17.57	17.63	17.72	17.84	17.98	18.11	18.25	18.37	18.49	18.59	18.68	18.75	18.81	18.86
15	17.79	17.81	17.86	17.94	18.04	18.15	18.26	18.38	18.49	18.59	18.68	18.76	18.83	18.89	18.93
20	18.01	18.03	18.07	18.14	18.22	18.31	18.41	18.51	18.60	18.69	18.77	18.85	18.91	18.96	18.99
25	18.20	18.23	18.27	18.32	18.39	18.46	18.54	18.63	18.71	18.79	18.86	18.92	18.98	19.02	19.05
30	18.38	18.40	18.44	18.48	18.54	18.60	18.67	18.74	18.81	18.88	18.94	18.99	19.04	19.08	19.10
35	18.54	18.56	18.59	18.63	18.68	18.73	18.79	18.85	18.90	18.96	19.01	19.06	19.10	19.13	19.14
40	18.68	18.70	18.73	18.76	18.80	18.84	18.89	18.94	18.99	19.03	19.07	19.11	19.14	19.17	19.18
45	18.80	18.82	18.84	18.87	18.91	18.94	18.98	19.02	19.06	19.10	19.13	19.16	19.18	19.20	19.20
50	18.90	18.92	18.94	18.97	19.00	19.03	19.06	19.09	19.12	19.15	19.17	19.19	19.21	19.22	19.22
55	18.99	19.01	19.03	19.05	19.07	19.09	19.12	19.14	19.16	19.18	19.20	19.22	19.23	19.23	19.23
60	19.05	19.07	19.09	19.11	19.12	19.14	19.16	19.18	19.19	19.21	19.22	19.23	19.23	19.23	19.22
65	19.10	19.11	19.13	19.14	19.16	19.17	19.18	19.20	19.21	19.21	19.22	19.22	19.22	19.22	19.21
70	19.12	19.14	19.15	19.16	19.17	19.18	19.19	19.20	19.20	19.20	19.21	19.21	19.20	19.20	19.19

Unit: mag arcsec^{-2} . $V_{\text{zen}} = 21.4$, $k = 0.23$, moon phase = 20° , hour angle = -30° , DEC = -10° , PA = 1.5 and PB = 0.90 .

Table 3 The sky brightness distribution when the moon's phase angle is 90° .

Dec\h	-35	-30	-25	-20	-15	-10	-5	0	5	10	15	20	25	30	35
-10	19.53	19.50	19.46	19.42	19.38	19.35	19.33	19.32	19.33	19.35	19.38	19.42	19.46	19.50	19.53
-5	19.55	19.50	19.45	19.39	19.34	19.29	19.26	19.24	19.26	19.29	19.34	19.39	19.45	19.50	19.55
0	19.56	19.50	19.43	19.35	19.28	19.21	19.16	19.14	19.16	19.21	19.28	19.35	19.43	19.50	19.56
5	19.56	19.49	19.40	19.31	19.21	19.11	19.04	19.01	19.04	19.11	19.21	19.31	19.40	19.49	19.56
10	19.57	19.48	19.38	19.26	19.14	19.01	18.90		18.90	19.01	19.14	19.26	19.38	19.48	19.57
15	19.58	19.48	19.37	19.23	19.08	18.92				18.92	19.08	19.23	19.37	19.48	19.58
20	19.59	19.49	19.38	19.24	19.08			Moon			19.08	19.24	19.38	19.49	19.59
25	19.62	19.52	19.41	19.28	19.13	18.97				18.97	19.13	19.28	19.41	19.52	19.62
30	19.66	19.57	19.47	19.35	19.23	19.11	19.02		19.02	19.11	19.23	19.35	19.47	19.57	19.66
35	19.71	19.63	19.54	19.45	19.36	19.27	19.21	19.19	19.21	19.27	19.36	19.45	19.54	19.63	19.71
40	19.76	19.70	19.63	19.56	19.49	19.43	19.39	19.38	19.39	19.43	19.49	19.56	19.63	19.70	19.76
45	19.82	19.77	19.72	19.67	19.62	19.58	19.55	19.55	19.55	19.58	19.62	19.67	19.72	19.77	19.82
50	19.88	19.84	19.81	19.77	19.74	19.71	19.69	19.69	19.69	19.71	19.74	19.77	19.81	19.84	19.88
55	19.94	19.91	19.89	19.86	19.84	19.82	19.81	19.81	19.81	19.81	19.82	19.84	19.86	19.89	19.91
60	19.99	19.97	19.95	19.94	19.92	19.91	19.91	19.90	19.91	19.91	19.92	19.94	19.95	19.97	19.99
65	20.03	20.02	20.01	20.00	19.99	19.99	19.98	19.98	19.98	19.98	19.99	19.99	20.00	20.01	20.03
70	20.07	20.06	20.06	20.05	20.05	20.04	20.04	20.04	20.04	20.04	20.05	20.05	20.06	20.06	20.07

Unit: mag arcsec^{-2} . $V_{\text{zen}} = 21.4$, $k = 0.23$, moon phase = 90° , hour angle = 0° , DEC = 20° , PA = 1.5 and PB = 0.90 .

the hour angle direction. In the declination direction, the sky brightness drops faster when pointing toward the zenith than toward the horizon.

5.2 Brightness Difference within a 5 Degree Field of View

The Large Sky Area Multi-Object Fiber Spectroscopic Telescope (LAMOST) is an optical survey telescope with a field of view of 5° . There are 16 spectrographs, each holding 250 fibers, and each spectrograph occupies a certain field of view (about 1°) on the LAMOST focal plane. In such a large

Table 4 Differences in brightness within LAMOST's field of view when the moon is over the zenith.

Dec\h	-35	-30	-25	-20	-15	-10	-5	0	5	10	15	20	25	30	35
-10	0.05	0.06	0.06	0.07	0.08	0.09	0.09	0.09	0.09	0.09	0.08	0.07	0.06	0.06	0.05
-5	0.06	0.07	0.08	0.10	0.10	0.11	0.11	0.11	0.11	0.11	0.10	0.10	0.08	0.07	0.06
0	0.08	0.09	0.10	0.12	0.13	0.13	0.14	0.14	0.14	0.13	0.13	0.12	0.10	0.09	0.08
5	0.09	0.11	0.12	0.14	0.15	0.16	0.16	0.16	0.16	0.16	0.15	0.14	0.12	0.11	0.09
10	0.11	0.12	0.14	0.16	0.17	0.18	0.23		0.23	0.18	0.17	0.16	0.14	0.12	0.11
15	0.12	0.14	0.15	0.17	0.19	0.29				0.29	0.19	0.17	0.15	0.14	0.12
20	0.13	0.15	0.17	0.19	0.20			Moon			0.20	0.19	0.17	0.15	0.13
25	0.13	0.15	0.17	0.19	0.21	0.36				0.36	0.21	0.19	0.17	0.15	0.13
30	0.13	0.15	0.17	0.19	0.21	0.23	0.26		0.26	0.23	0.21	0.19	0.17	0.15	0.13
35	0.13	0.15	0.17	0.18	0.20	0.21	0.22	0.23	0.22	0.21	0.20	0.18	0.17	0.15	0.13
40	0.13	0.14	0.16	0.17	0.18	0.19	0.20	0.20	0.20	0.19	0.18	0.17	0.16	0.14	0.13
45	0.12	0.14	0.15	0.16	0.17	0.18	0.18	0.18	0.18	0.18	0.17	0.16	0.15	0.14	0.12
50	0.11	0.12	0.13	0.14	0.15	0.16	0.16	0.16	0.16	0.16	0.15	0.14	0.13	0.12	0.11
55	0.10	0.11	0.12	0.13	0.13	0.14	0.14	0.14	0.14	0.14	0.13	0.13	0.12	0.11	0.10
60	0.09	0.10	0.11	0.11	0.11	0.12	0.12	0.12	0.12	0.12	0.11	0.11	0.11	0.10	0.09
65	0.08	0.08	0.09	0.09	0.10	0.10	0.10	0.10	0.10	0.10	0.10	0.09	0.09	0.08	0.08
70	0.07	0.07	0.07	0.08	0.08	0.08	0.08	0.08	0.08	0.08	0.08	0.08	0.07	0.07	0.07

Unit: mag arcsec⁻². $V_{\text{zen}} = 21.4$, $k = 0.23$, moon phase = 20°, hour angle = 0°, DEC = 20°, PA = 1.5 and PB = 0.90.

field of view, the gradient of the background cannot be ignored. In most observations of spectra taken with fibers, the sky is sampled by dedicated fibers, then the sky in the fiber with the target object is subtracted using a spectrum taken from those sky fibers. This step works well when the sky is homogenous within the field of view of the spectrograph. In the case of a moon night, the gradient of the sky background should be considered in the data reduction step as well as in the step that plans how the fiber samples the background. In this work, we try to estimate the difference in brightness caused by moonlight within the field of view of LAMOST, so as to provide a reference for strategy decisions related to observations as well as data reduction. From Tables 2 and 3, it is easy to tell that the larger the angular separation is, the lower the gradient of the sky brightness is. To calculate the maximum difference in brightness within the field of view, we need to find the points with the maximum and minimum brightness. The points with an extreme value were found by a step-by-step search along the edge of the field of view.

We show an example of the results in Table 4. The input parameters are the same as in Table 3 except that the phase angle of the moon is 20° rather than 90°. Each item in Table 4 is the maximum difference in LAMOST's 5° field of view. The maximum difference in Table 4 is 0.36 mag/5°, so in the field of view of one of LAMOST's spectrographs (about 1°), the gradient will be about 0.07 mag, which means the gradient in each spectrograph is 7%. This will cause residuals from sky subtraction in the data reduction if the sky is not properly sampled. However, the smallest difference in the table is about 0.05 mag, which means there is about a 1% gradient in one spectrograph. Generally, the accuracy in sky subtraction in spectral data reduction from the fiber is larger than 2%, so a difference of 1% can be acceptable in most cases. From the above discussion, it is better to choose a position with a smaller background gradient to alleviate difficulty in data reduction when planning a survey like LAMOST.

Figure 9 shows an example of sky brightness distribution inside LAMOST's 5° field of view. We calculate the brightness for each fiber. The phase angle of the moon is 20°, and the distance between the moon and the center of the field is about 30° as marked in the figure. The moon is 67° to the northeast, as shown by the lower right icon. As we can see, there is a brightness gradient of about 0.16 mag, but the direction of the gradient is not the direction from the moon to the sky position. As we pointed out in Section 5.1, this is because when the airmass increases going away

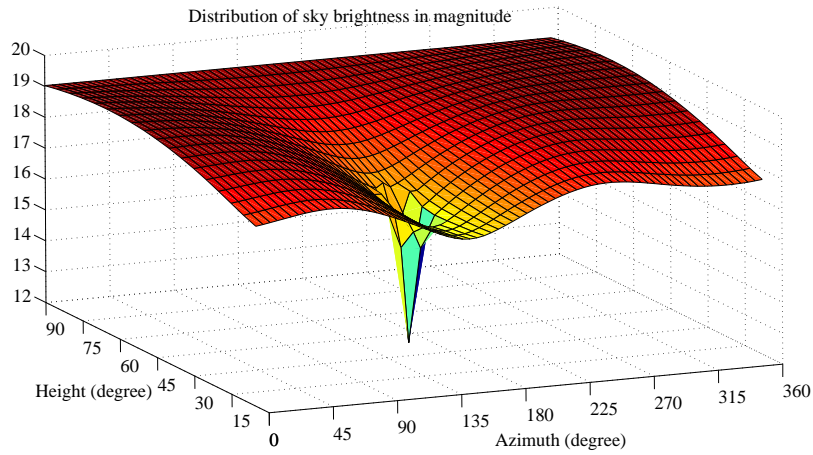


Fig. 8 Distribution of sky brightness in magnitude; the input parameters are: $V_{zen} = 21.4$, $k = 0.23$, Moon phase = 20° , DEC = -20° , hour angle = -30° , PA = 1.5 and PB = 0.90.

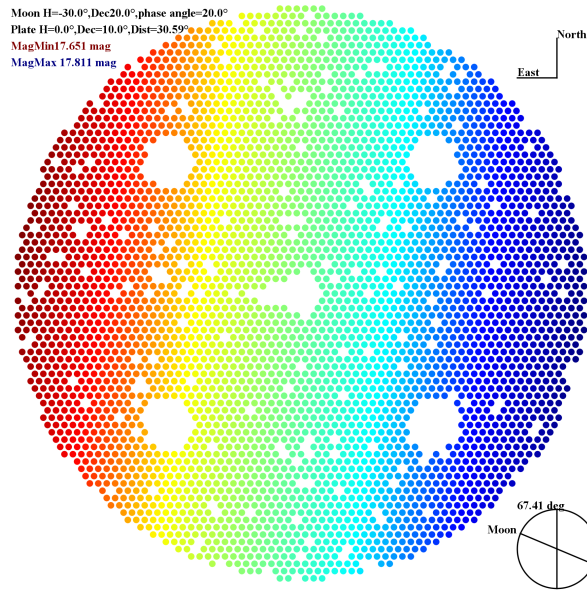


Fig. 9 Simulation of brightness distribution in LAMOST's focal plate. The moon is 2 hours before the zenith and the declination is 20° . The telescope is pointing towards the meridian with a declination of 10° . PA = 1.5, PB = 0.90, $V_{zen} = 21.4$, $k = 0.23$ and moon phase angle $\alpha = 20^\circ$. The location of fibers is assumed to be placed in the sky by following their light path to make the figure more intuitive. Due to the factor related to the zenith distance of the sky position, the direction of the moon does not match the direction of the brightness gradient. The direction of increasing brightness slightly shifts from the moon to the horizon. The variation becomes larger at the horizon.

from the zenith (i.e. north in this figure), the moonlight becomes more scattered by the atmosphere, which will change the direction of gradient a bit to the south.

6 SUMMARIES

We use an SQM to study the brightness of the night sky at the Xinglong station. Using data collected from December 2010 to March 2012, we selected 22 dark clear nights to study how the sky brightness varies with time. We found a clear correlation between the dark nighttime sky brightness and human activity. We also utilize the lunar sky brightness model of Krisciunas & Schaefer (1991), by modifying the relative scale factors of Rayleigh and Mie scattering. We successfully fitted the sky brightness data of the SQM at the Xinglong station with an RFV of 12%. We estimate the related parameters for 90 nights. According to the results we can see that in this observatory the typical V band dark zenith sky brightness is about 21.4 mag arcsec⁻²; the extinction coefficient is about 0.23; the Mie scattering scale factor is about 1.5; the Rayleigh scattering scale factor is about 0.90. With the model and those typical parameters for the Xinglong station, we could estimate the sky brightness distribution for any given time during a moon night for the LAMOST site. We then calculated the gradient within LAMOST's 5° field of view. The result shows that sky brightness increases quickly as the distance from the moon becomes smaller. The increasing zenith distance will also enhance the brightness within a quantity much smaller than the influence of the lunar separation angle. These results will help in planning the LAMOST bright night survey by determining good locations for sky fibers in the focal plane as well as data reduction used in the LAMOST survey.

Acknowledgements The authors thank Qiu Peng and Lu Xiaomeng for helping to get the SQM data and related information. The authors also thank the referee for useful suggestions. The Guo Shou Jing Telescope (the Large Sky Area Multi-Object Fiber Spectroscopic Telescope; LAMOST) is a National Major Scientific Project built by the Chinese Academy of Sciences. Funding for the project has been provided by the National Development and Reform Commission. LAMOST is operated and managed by the National Astronomical Observatories, Chinese Academy of Sciences.

References

- Chakraborty, P., Das, H. K., & Tandon, S. N. 2005, *Bulletin of the Astronomical Society of India*, 33, 513
- Cinzano, P. 2005, *UISTIL Internal Report*, 9, <http://www.lightpollution.it/download/sqmreport.pdf>
- Cui, X.-Q., Zhao, Y.-H., Chu, Y.-Q., et al. 2012, *RAA (Research in Astronomy and Astrophysics)*, 12, 1197
- Garstang, R. H. 1989, *PASP*, 101, 306
- Krisciunas, K., & Schaefer, B. E. 1991, *PASP*, 103, 1033
- Liu, Y., Zhou, X., Sun, W.-H., et al. 2003, *PASP*, 115, 495
- Meeus, J. 1991, *Astronomical Algorithms* (Willmann-Bell, Incorporated)
- Neugent, K. F., & Massey, P. 2010, *PASP*, 122, 1246
- Sánchez, S. F., Aceituno, J., Thiele, U., Pérez-Ramírez, D., & Alves, J. 2007, *PASP*, 119, 1186
- Schneeberger, T. J., Worden, S. P., & Beckers, J. M. 1979, *PASP*, 91, 530
- Yao, S., Liu, C., Zhang, H.-T., et al. 2012, *RAA (Research in Astronomy and Astrophysics)*, 12, 772